

Letters

Friction stir lap weld-brazing of AA7050 aluminium alloy to Ti6Al4V titanium alloy – Limitations in dissimilar metal joining

Felix Grassel ^{a,*}, Benjamin Klusemann ^{a,b}^a Solid State Materials Processing, Institute of Material and Process Design, Helmholtz-Zentrum Hereon, Max-Planck-Strasse 1, 21502 Geesthacht, Germany^b Institute for Production Technology and Systems, Leuphana University Lüneburg, Universitätsallee 1, 21335 Lüneburg, Germany

ARTICLE INFO

Article history:

Received 24 December 2024

Received in revised form 1 March 2025

Accepted 18 March 2025

Available online 7 May 2025

Keywords:

Friction Stir Welding

Interface

Temperature

Mechanical Properties

ABSTRACT

Joining of high-strength aluminium and titanium alloys gives new opportunities for cost- and energy-efficient designs especially in the transportation industry. In the present study, friction stir lap joining of AA7050 and Ti6Al4V was conducted, investigating the thermal cycle in the interface via variation of energy input by the spindle rotation rate. Temperature measurements reveal that the interface temperature exceeds the solidus temperature of the aluminium alloy and reached up to 570 °C, so that the process should be classified as semi-solid-state. Additionally, no indication for intermetallic compounds was found. Lap-shear strength of the joint is found to be limited by low diffusion kinetics at low temperatures and liquation cracking at high temperatures, revealing clear indications for the limitations of this specific material combination for the first time.

© 2025 The Authors. Published by Elsevier Ltd on behalf of Society of Manufacturing Engineers (SME). This is an open access article under the CC BY license (<http://creativecommons.org/licenses/by/4.0/>).

1. Introduction

Friction Stir Welding (FSW) is a promising solid-state welding process [1] that has proven to be able to join material combinations which have previously been considered unweldable, like aluminium to copper [2], to steel [3], to polymers [4] and to titanium [5]. Latter is of special interest for aeronautical applications. However, welding Al to Ti is challenging because of the materials' diverging properties, albeit extensive efforts have been made [6]. With the solidus temperature of Ti being more than 1000 K higher than that of Al, a complex system of brittle intermetallic compounds (IMC) [7] is formed during fusion welding, resulting in poor weld quality [8]. Solid-state techniques can overcome these issues to a certain extent by mitigating the IMC formation. Still, sufficient energy input is required to achieve diffusive bonding [9]. In principle, there are three approaches for FSW of Al to Ti: Butt welding, where the tool probe is inserted into the interface between Ti on the advancing (AS) and Al on the retreating side (RS) [10], lap welding, where the tool probe plunges through the Al sheet into the Ti [11] and lap joining, where the tool only plasticises the Al and is just scratching or not even touching the Ti surface [12]. Technically, only the latter leads to a solid-state joining process, as the

other two will lead to partial melting of Al. FSW has been proven to be able to joint Al and Ti with strength up to 100 % of the Al base material for pure Al [13], AlMg-alloys [14] and AlMgSi-alloys [15].

High strength to weight ratio is crucial for aircraft materials, where Al-Cu alloys (2xxx series) and especially Al-Cu-Zn alloys (7xxx series) as well as Ti6Al4V are commonly utilised. While several investigations regarding FSW of Al-Cu alloys to Ti are published [11,16–18], the joining of Al-Cu-Zn alloys to Ti is scarcely described – for reasons, as will be concluded later. Aonuma and Nakata [19] compared butt-welding of AA2024 and AA7075 to Ti/Ti6Al4V and found AA7075 welds less firm. Ugurlu and Cakan [20] achieved a maximum tensile strength of below 40 % of AA7075 when welding it to Ti6Al4V, while Österreicher et al. [21] applied post-weld heat-treatment, which increased the tensile strength by 15 %. Dias et al. [13] added conical holes in the Ti sheet which were filled with Al during the welding process generating additional mechanical interlocking. To best of the authors knowledge, there is only one specific investigation on joining of AA7050 to Ti6Al4V [22]. In this case, insert moulding was used and Al was heated up to 700–790 °C – far above the solidus temperature, resulting in a lap-shear strength of 154 MPa, i.e. far lower than the base metal strength. The aim of this investigation is to reveal the thermal cycle in the interface and its impact on the interface evolution and mechanical properties, providing indications of limitation in reachable properties of AA7050/ Ti6Al4V joints.

* Corresponding author.

E-mail addresses: felix.grassel@hereon.de (F. Grassel), benjamin.klusemann@hereon.de (B. Klusemann).

2. Materials and Methods

Sheets of AA7050 of 2 mm were lap-joined to Ti6Al4V sheets of same thickness. All dimensions are shown in Fig. 1. Joints with a length of 470 mm (for strength investigation) and 350 mm (for interface temperature measurements) were produced on a custom-designed gantry FSW-machine. The tool consists of a scrolled planar shoulder, 15 mm in diameter and a tri-flat threaded probe, 12° conical, with a base diameter of 6 mm and a length of 2 mm, see Fig. 2a), made of hot-work tool steel (HOTVAR®).

The welding speed and process force were 2.5 mm/s and 8kN, respectively, leading to defect-free welds for a suitable range of rotational speeds (RotS), varied between 600 and 1300 rpm. Process forces and torque were recorded. Tool temperature was measured via a K-type thermocouple (T_{TC}) inserted in the tool, see Fig. 2a). Additionally, temperatures at the interface (T_{Interf}) were determined via three K-type thermocouples inserted into suitable grooves at the Ti surface, which were milled for this purpose. The interface temperatures were measured 5 mm to the RS and AS, as well as at the centre of the joint line, each 10 mm apart from each other, see Fig. 1.

For each parameter set, three lap-shear samples with a width of 30 mm were extracted. A universal testing machine (Zwick) at a constant travel-speed of 1 mm/min was employed. Cross-sections were cut out of each weld, metallographically prepared and investigated under optical (OM, Keyence VHX-6000) as well as scanning electron microscopes (SEM, Quanta FEG450).

3. Results

The tool temperature showed an asymptotic trend caused by the heat flux into the spindle, so the maximum reached temperature was chosen for comparison, Fig. 2a). An almost linear increase of maximum tool temperature with increasing RotS is detected, which shows no evidence of asymptotic towards the aluminium solidus temperature (490 °C), assuming to be the limiting temperature for the process. For 600 rpm, the maximum temperature deviates from this trend, as the process was unstable due to insufficient heat generation.

Analysing the process torque, Fig. 2b), a roughly asymptotic decrease with increasing RotS is observed, which indicates softening of the material with increasing process temperatures. A noticeable decrease in torque is measured between 1100 and 1200 rpm indicating a change in the material behaviour, presumably due to

partial melting. In contrast, the average energy per unit length, Fig. 2c), is rather constant around 330 J/mm up to 900 rpm but increases to 370 J/mm for higher RotS. This might indicate the appearance of liquation within the material that consumes additional energy [23].

The interfacial temperature, Fig. 1, shows a steep increase as the tool approaches the measurement position, followed by a short plateau, corresponding to the probe contact time and a decay afterwards, where cooling rate is much lower than heating rate, with maximum temperature in the weld centreline. Expectedly, the temperature is higher on the AS [24]. The peak interfacial temperature, Fig. 2d), rises approximately linear with RotS from 490 to 535 °C, i.e. temperatures above the solidus temperature of AA7050. Therefore, in all processes the solidus temperature of AA7050 was at least reached. The higher the peak temperature, the higher is the remaining heat behind the tool when the plasticised aluminium gets in contact with the titanium surface. Consequently, partial melting of at least a thin layer of aluminium must be assumed.

No volumetric defects or significant Ti particles were found in Al, however, for larger RotS than 1000 rpm, liquation cracks become visible in the upper half of the Al sheet, Fig. 3a). The bonding zone shows a width of around 5.5–6 mm corresponding to the probe diameter. The analyses via SEM reveal that the Ti surface becomes rougher with increasing RotS. Close to the Ti interface, void defects at the Al grain boundaries, Fig. 3d), become visible. Additionally, Ti flakes in the micrometre range are seen close to the interface, Fig. 3c). There was no indication of the formation of IMCs.

Elemental mapping was performed to search for agglomeration or depletion of certain elements close to the interface. While there was no indication of IMCs (plateau in the Al-Ti interface), agglomeration of magnesium and zinc at the grain boundaries is visible, Fig. 3d). Voids are found close to these agglomerations, leading to the assumption of liquation cracking, as also found for similar FSW of AA7050 [25].

In term of lap-shear strength, the value was very low for 600 rpm, while with increasing RotS the mechanical strength increases, Fig. 4a). This is reasonable as higher temperatures during the process promote the interdiffusion of Al and Ti. The highest lap-shear strength of 381 N/mm was found for 1100 rpm. Above this RotS, strength decreased drastically. As there was no brittle IMC detectible, this is believed to be caused by the overheating of Al close to the interface, supported by the element analysis, indicating liquation cracking.

4. Discussion and Conclusions

In contrast to investigations using Friction-Stir-Lap-Weld-Brazing for Al-Mg-Si alloys [26], no intermediate layer was detectible in joining of AA7050 to Ti6Al4V, which is in accordance with findings for Al-Cu-Zn alloys [21]. This is believed to be caused by the lower solidus temperature of AA7050 and therefore lower process temperatures. As diffusion is depending on time, temperature and plastic deformation, the time that the material at the interface stays above certain temperatures is calculated, Fig. 4b). The holding time at 475 °C, i.e. below the Al solidus, is increasing almost linear with RotS. In contrast, the 500 °C level time increases steeper between 700 and 1000 rpm but reaches a plateau that corresponds to the time the probe tip is in contact with the interface, roughly 2 s. For these conditions, the highest lap-shear strength was reached. With further increase in RotS, the interface surpasses 525 °C and the time above the solidus temperature increases. In this case, it can be assumed that solidification defects, such as liquation cracking, reduce the mechanical properties of the bond.

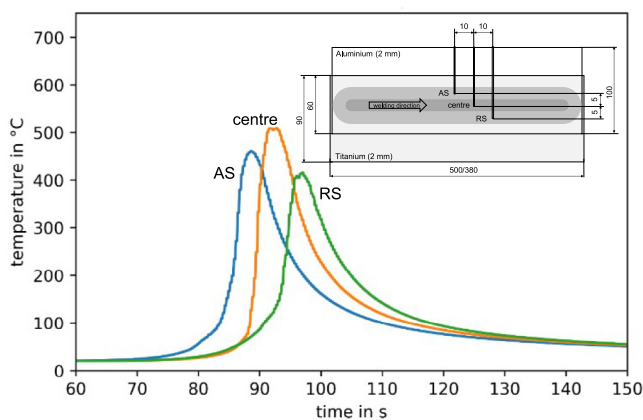


Fig. 1. Evolution of interface temperature on AS, RS, and at centre, exemplarily shown for 1000 rpm, including sample setup with thermocouple-positioning for measuring T_{Interf} . All dimensions in mm.

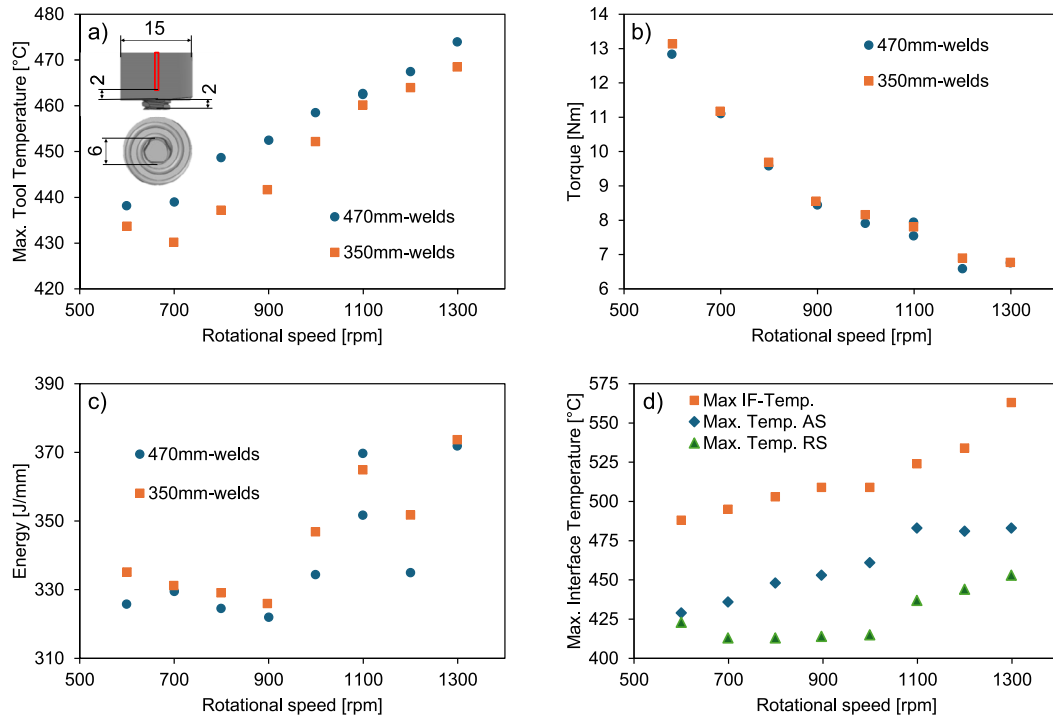


Fig. 2. a) Measured maximum temperature within the tool over rots, b) recorded average tool torque over rots and c) calculated average energy input per unit length over rots, where data are obtained from two sets of experiments (470 mm-welds and 350 mm-welds). d) Recorded peak interface temperatures over RotS during interface temperature welds.

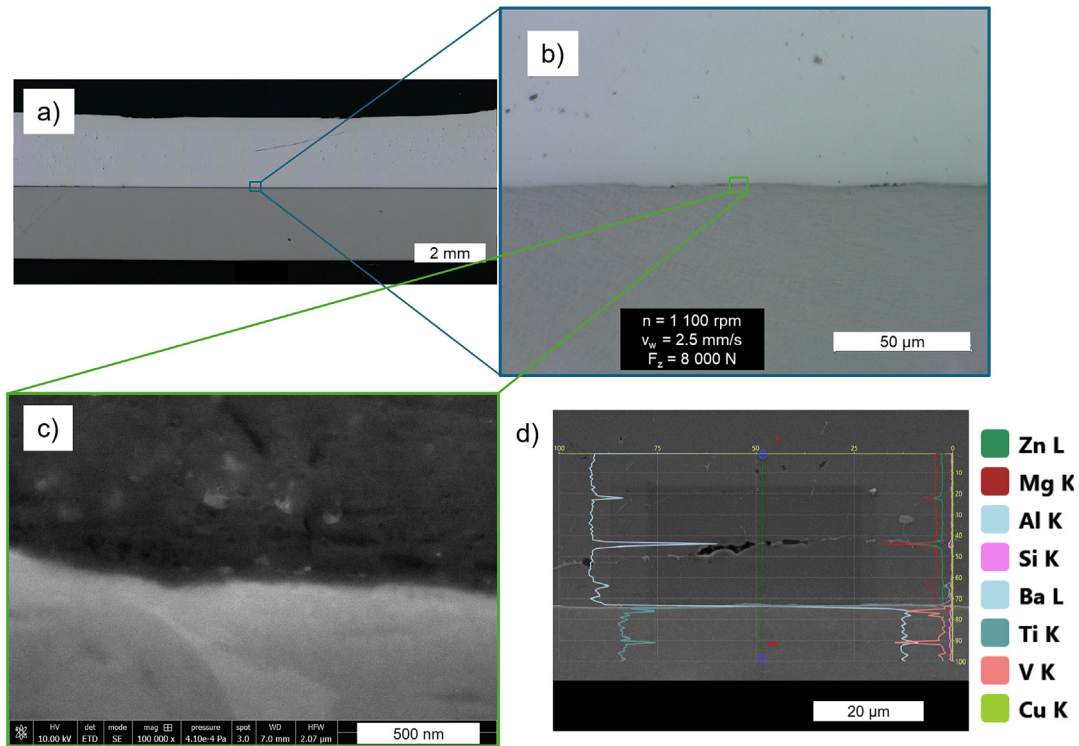


Fig. 3. Cross-section of the interface in the centre of the weld for RotS of 1100 rpm in a) low and b) high magnification via OM, showing cracks in the stir zone but no indications of bonding mechanism. c) High-magnification SEM image of the interface for RotS of 1100 rpm shows roughened surface. d) Elemental line scan through the interface at the weld centreline at 1200 rpm displays agglomeration of Mg and Zn as well as volumetric defects in the grain boundaries close to the interface.

From diffusion welding, it is known that diffusion between Al and Ti becomes significant above 520–550 °C [27]. Plastic deformation enhances the diffusion [28] and consequently lowers the dif-

fusion time and temperature. Therefore, interdiffusion can be believed to start around 450 °C, explaining a bond formation at lower RotS. However, the diffusion kinetics and therefore bond

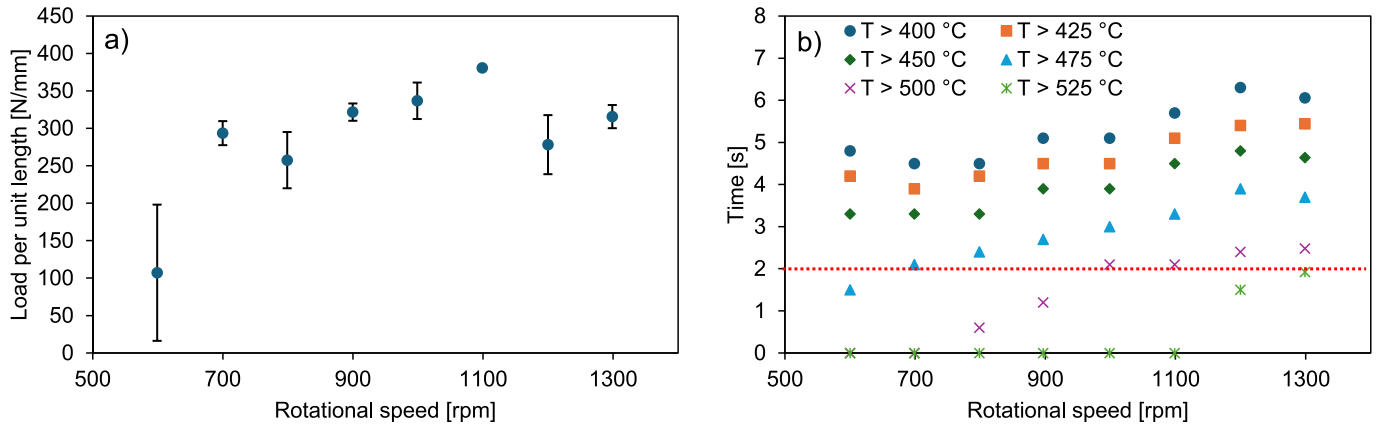


Fig. 4. a) Lap-shear load per unit length over RotS and b) time of the interface temperature staying above a certain level over RotS. Tool passing time is indicated by dotted line.

strength is still low, but a further increase of the process times increases distortion and residual stresses. Increasing process temperature instead additionally leads to liquation cracking also deteriorating mechanical properties. Another approach is to activate the titanium by plastic deformation [21], however, in this case the temperature will be most likely above the Al solidus. Additionally, plasticising Ti causes increased tool wear.

Therefore, it might be concluded that physical limitations, i.e. diffusion kinetics of Al–Ti, the solidus temperature of AA7050 and the plastification temperature of Ti6Al4V do not allow for a ductile and high-strength joining of Al–Cu–Zn alloys, especially AA7050, to Ti6Al4V via FSW.

CRediT authorship contribution statement

Felix Grassel: Writing – review & editing, Writing – original draft, Visualization, Methodology, Investigation, Data curation, Conceptualization. **Benjamin Klusemann:** Writing – review & editing, Supervision, Methodology, Funding acquisition, Formal analysis.

Declaration of competing interest

The authors declare that they have no known competing financial interests or personal relationships that could have appeared to influence the work reported in this paper.

References

- Mishra RS, Ma ZY. Friction stir welding and processing. *Mater Sci Eng R Rep* 2005;50(1–2):1–78. <https://doi.org/10.1016/j.mser.2005.07.001>.
- Isa MSM, Moghadasi K, Ariffin MA, Raja S, Muhamad MRB, Yusof F, et al. Recent research progress in friction stir welding of aluminium and copper dissimilar joint: a review. *J Mater Res Technol* 2021;15:2735–80. <https://doi.org/10.1016/j.jmrt.2021.09.037>.
- Beygi R, Galvão I, Akhavan-Safar A, Pouraliakbar H, Fallah V, da Silva LFM. Effect of alloying elements on intermetallic formation during friction stir welding of dissimilar metals: a critical review on aluminum/steel. *Metals* 2023;13(4):768. <https://doi.org/10.3390/met13040768>.
- Haghshenas M, Khodabakhshi F. Dissimilar friction-stir welding of aluminum and polymer: a review. *Int J Adv Manuf Technol* 2019;104(1–4):333–58. <https://doi.org/10.1007/s00170-019-03880-2>.
- Simar A, Avettand-Fènoël M-N. State of the art about dissimilar metal friction stir welding. *Sci Technol Weld Join* 2017;22(5):389–403. <https://doi.org/10.1080/13621718.2016.1251712>.
- Gadakh VS, Badheka VJ, Mulay AS. Solid-state joining of aluminum to titanium: a review. *Proce Institution of Mechanical Engineers, Part L: J. Materials: Design and Applications* 2021;235(8):1757–99. <https://doi.org/10.1177/14644207211010839>.
- Sujata M, Bhargava S, Sangal S. On the formation of TiAl₃ during reaction between solid Ti and liquid Al. *J Mater Sci Lett* 1997;16(14):1175–8. <https://doi.org/10.1007/BF02765402>.
- Vaidya WV, Horstmann M, Ventzke V, Petrovski B, Koçak M, Kocik R, et al. Structure-property investigations on a laser beam welded dissimilar joint of aluminium AA6056 and titanium Ti6Al4V for aeronautical applications Part I: Local gradients in microstructure, hardness and strength. *Mat-wiss u Werkstofftech* 2009;40(8):623–33. <https://doi.org/10.1002/mawe.200900366>.
- Wilden J, Bergmann JP. Manufacturing of titanium/aluminium and titanium/steel joints by means of diffusion welding. *Weld Cut* 2004;56(5):285–90.
- Choi J-W, Liu H, Fujii H. Dissimilar friction stir welding of pure Ti and pure Al. *Mater Sci Eng A* 2018;730(5):168–76. <https://doi.org/10.1016/j.msea.2018.05.117>.
- Geyer M, Vidal V, Pottier T, Boher C, Rézaï-Aria F. Investigations on the material flow and the role of the resulting hooks on the mechanical behaviour of dissimilar friction stir welded Al2024-T3 to Ti-6Al-4V overlap joints. *J Mater Process Technol* 2021;292:117057. <https://doi.org/10.1016/j.jmatprotec.2021.117057>.
- Krutzlinger M, Marstatt R, Suenger S, Luderschmid J, Zaeh MF, Haider F. Formation of joining mechanisms in friction stir welded dissimilar Al-Ti lap joints. *AMR* 2014;966–967:510–20. <https://doi.org/10.4028/www.scientific.net/AMR.966-967.510>.
- Dias F, Cipriano G, Correia AN, Braga DFO, Moreira P, Infante V. Joining of aluminum alloy AA7075 and titanium alloy Ti-6Al-4V through a friction stir welding-based process. *Metals* 2023;13(2):249. <https://doi.org/10.3390/met13020249>.
- Rostami H, Nourouzi S, Jamshidi AH. Analysis of welding parameters effects on microstructural and mechanical properties of Ti6Al4V and AA5052 dissimilar joint. *J Mech Sci Technol* 2018;32(7):3371–7. <https://doi.org/10.1007/s12206-018-0640-8>.
- Bang H-S, Bang H, Song H, Joo S. Joint properties of dissimilar Al6061-T6 aluminum alloy/Ti-6%Al-4%V titanium alloy by gas tungsten arc welding assisted hybrid friction stir welding. *Mater Des* 2013;51:544–51. <https://doi.org/10.1016/j.matdes.2013.04.057>.
- Buffa G, de Lisi M, Sciortino E, Fratini L. Dissimilar titanium/aluminum friction stir welding lap joints by experiments and numerical simulation. *Adv Manuf* 2016;4(4):287–95. <https://doi.org/10.1007/s40436-016-0157-2>.
- Dressler U, Biallas G, Alfaro MU. Friction stir welding of titanium alloy TiAl6V4 to aluminium alloy AA2024-T3. *Mater Sci Eng A* 2009;526(1–2):113–7. <https://doi.org/10.1016/j.msea.2009.07.006>.
- Kar A, Suwas S, Kailas SV. Two-pass friction stir welding of aluminum alloy to titanium alloy: a simultaneous improvement in mechanical properties. *Mater Sci Eng A* 2018;733:199–210. <https://doi.org/10.1016/j.msea.2018.07.057>.
- Aonuma M, Nakata K. Dissimilar metal joining of 2024 and 7075 aluminium alloys to titanium alloys by friction stir welding. *Mater Trans* 2011;52(5):948–52. <https://doi.org/10.2320/matertrans.L-MZ201102>.
- Ugurlu M, Cakan A. Dissimilar friction stir butt welding of AA7075-T6 Al and Ti6Al4V Ti plates: mechanical and metallurgical analysis. *Int J Adv Manuf Technol* 2023;128(7–8):3491–506. <https://doi.org/10.1007/s00170-023-12114-5>.
- Österreicher JA, Pfeiffer C, Kunschert G, Weinberger T, Schlögl CM, Suppan W, et al. Dissimilar friction stir welding and post-weld heat treatment of Ti-6Al-4V and AA7075 producing joints of unprecedented strength. *J Adv Joining Processes* 2024;9(5):100213. <https://doi.org/10.1016/j.jaip.2024.100213>.
- Li H, Nie X, He Z, Zhao K, Du Q, Zhang J, et al. Interfacial microstructure and mechanical properties of Ti-6Al-4V/Al7050 joints fabricated using the insert molding method. *Int J Miner Metall Mater* 2017;24(12):1412–23. <https://doi.org/10.1007/s12613-017-1534-y>.
- Li P-Y, Xiong B-Q, Zhang Y-A, Li Z-H. Temperature variation and solution treatment of high strength AA7050. *Trans Nonferrous Met Soc Chin* 2012;22(3):546–54. [https://doi.org/10.1016/S1003-6326\(11\)61212-0](https://doi.org/10.1016/S1003-6326(11)61212-0).
- Silva ACF, de Backer J, Bolmsjö G. Temperature measurements during friction stir welding. *Int J Adv Manuf Technol* 2017;88(9–12):2899–908. <https://doi.org/10.1007/s00170-016-9007-4>.

- [25] Sun T, Reynolds AP, Roy MJ, Withers PJ, Prangnell PB. The effect of shoulder coupling on the residual stress and hardness distribution in AA7050 friction stir butt welds. *Mater Sci Eng A* 2018;735:218–27. <https://doi.org/10.1016/j.msea.2017.12.018>.
- [26] Kalinenko A, Dolzhenko P, Malopheyev S, Yuzbekova D, Borisova Y, Shishov I, et al. Interfacial microstructure produced during dissimilar AA6013/Ti-6Al-4V friction stir lap welding under zero-penetration condition. *Metals* 2023;13(10):1667. <https://doi.org/10.3390/met13101667>.
- [27] Wilden J, Bergmann JP, Jahn S. Mechanical properties and processing of low-temperature diffusion-welded hybrid joints. *Adv Eng Mater* 2006;8(3):212–8. <https://doi.org/10.1002/adem.200600006>.
- [28] Kar A, Suwas S, Kailas SV. Multi-Length scale characterization of microstructure evolution and its consequence on mechanical properties in dissimilar friction stir welding of titanium to aluminum. *Metall and Mat Trans A* 2019;50(11):5153–73. <https://doi.org/10.1007/s11661-019-05409-4>.